Genesis on-board determination of the solar wind flow regime

M.Neugebauer
Jet Propulsion Laboratory, California Institute of Technology, Pasadena, California

J. T. Steinberg, R. L. Tokar, B. L. Barraclough, E. E. Dors, and R. C. Wiens
Los Alamos National Laboratory, Los Alamos, New Mexico

D. E. Gingerich and D. Luckey
Lockheed Martin Astronautics, Denver, Colorado

D. B. Whiteaker
Raytheon Missile Systems, Tucson, Arizona

15 May, 2002

Abstract. Some of the objectives of the Genesis mission require the separate collection of solar wind originating in different types of solar sources. Measurements of the solar wind protons, alpha particles, and electrons are used on-board the spacecraft to determine whether the solar-wind source is most likely a coronal hole, interstream flow, or a coronal mass ejection. A simple fuzzy logic scheme operating on measurements of the proton temperature, the alpha-particle abundance, and the presence of bidirectional streaming of suprathermal electrons was developed for this purpose. Additional requirements on the algorithm include the ability to identify the passage of forward shocks, reasonable levels of hysteresis and persistence, and the ability to modify the algorithm by changes in stored constants rather than changes in the software. After a few minor adjustments, the algorithm performed well during the initial portion of the mission.

Keywords: Genesis mission, solar wind

1. Introduction

The purpose of the Genesis mission is to determine the elemental and isotopic compositions of the outer layers of the Sun. The method used is to collect samples of the solar wind and return those samples to Earth for detailed analyses in state-of-the-art laboratories (Burnett *et al.*, 2002) . But although the solar wind originates in the outer layers of the Sun, some change in composition (fractionation) occurs during the processes of removing that material from the Sun and accelerating it into the solar wind. The strength and nature of the fractionation are not constant, but depend on the variable properties of the solar wind. These variations are best characterized by considering three different types, or regimes, of solar-wind flow. There are two types of quasi-

stationary solar wind — the high-velocity streams from the cooler, less dense regions of the solar atmosphere called coronal holes (CH) and the slower interstream (IS) flow observed between successive CH streams. The quasi-stationary CH and IS flows are occasionally interrupted by the transient injection of new material into the solar wind in explosive events called coronal mass ejections (CME). CMEs occur more frequently at high activity phases of the solar cycle than at solar minimum.

Elemental fractionation of the solar wind depends largely on the time required for an element to become ionized in the solar atmosphere. The ionization time, in turn, is most strongly influenced by an element's first-ionization potential (FIP = the energy required to remove one electron from an atom). The elemental fractionation due to the FIP effect is observed to be much greater in IS than in CH flow; in IS wind, low-FIP elements are enhanced compared to high-FIP elements by a factor of 4 to 5, whereas the enhancement factor is $\leqslant 2$ for CH wind (von Steiger *et al.*, 2000). A second, much weaker source of fractionation is Coulomb drag close to the Sun where the solar wind still undergoes collisions; this source of fractionation depends on the mass/charge ratio of the ions. Because each isotope of an element has the same FIP, the isotopic fractionation is expected to be much less than the elemental fractionation, and may even be negligible in the quasi-stationary solar wind. The fractionation properties of the CME wind are much more variable than those of the CH and IS winds. Large enhancements of the ^{3}He:^{4}He isotope ratio have been observed in several CME events (Gloeckler *et al.*, 1999; Ho *et al.*, 2000). Elemental abundance ratios are also highly variable in CMEs (Galvin, 1997).

To be able to correct for elemental fractionation and to test for any isotopic fractionations in elements heavier than He, Genesis will expose different collectors to CH, IS, and CME solar wind. The challenge is to determine the correct regime in real-time from the information provided by the Genesis solar wind monitors (described in the paper by Barraclough *et al.*, 2002). This paper describes the on-board algorithm developed to make such a determination. Section 2 explains the logic of the algorithm. Section 3 describes the method of calculating the parameters needed as input to the algorithm, while Section 4 provides some insight into the performance of the algorithm during the first few months after launch.

2. The Algorithm

The data available as input to the regime-selection algorithm are obtained by the Genesis Ion Monitor (GIM) and the Genesis Electron Monitor (GEM). The design and operation of the two monitors are described in the companion paper by Barraclough *et al.*(2002). Ideally, the identification of solar-wind regimes would be based not only on the parameters that can be measured by GIM and GEM, but also on data from other types of instruments, such as a magnetometer, an ion mass spectrometer, and energetic particle detectors. But there are several identifying characteristics of each regime that are within the capability of the instrumentation on Genesis. Coronal hole (CH) wind is characteristically fast (speed > 500 km/s) and hot (proton temperature $\leq$ 1-2$\times 10^5$ K); it has a generally steady helium abundance of 4 to 5%; and suprathermal electrons stream outward from the Sun along the interplanetary magnetic field. Interstream (IS) wind is slower (speed usually < 450 km/s) and cooler (proton temperature $\leq 10^5$ K) than the CH wind; its helium abundance is generally lower (0 – 4%) and more variable; and suprathermal electrons usually flow away from the Sun, but sometimes they are absent. The coronal mass ejection (CME) wind can have any speed; its proton temperature is often anomalously low due to the 3-dimensional expansion as the ejecta flow away from the Sun; its helium abundance is sometimes strongly enhanced (8 – 30%); and suprathermal electrons often stream in both directions along the magnetic field, which is believed to indicate that the field has the form of a large loop anchored in the Sun.

Reflecting these nominal properties of the different flow types, the regime algorithm is based on estimates of the following plasma parameters calculated following each 2.5-minute GIM/GEM data cycle:

V_p = proton speed
N_p = proton number density
T_p = proton temperature
N_a = alpha-particle number density
B_e = measure of bidirectional electron streaming

The detailed definitions and the method of calculating these parameters are described in Section 3.

In addition to the capabilities and constraints provided by GIM and GEM, there are several additional requirements on the regime algorithm. First the number of regime changes must be minimized consistent with the goal of collecting sufficiently pure samples of each regime. The motors that run the array-changing mechanisms have a design requirement of 400 regime changes over the course of the mission, although the motors are expected to last much longer than that. Fur-

thermore, each array change requires up to 6 minutes to implement and can disturb the pointing of the spacecraft for up to an hour. This low-change-rate requirement means that the algorithm should have both hysteresis and persistence. A second requirement is that the algorithm should be biased toward minimizing the contamination of the CH sample by CME or IS wind; the CH sample is given special protection because its composition is expected to be less fractionated than the IS and CME winds. A third requirement is that the algorithm be adjustable largely by changing numerical parameters in look-up tables as opposed to uploading new software.

The first step in determining the correct regime is to form running averages of the parameters V_p, T_{ex}/T_p, N_a/N_p, and B_e. The nominal averaging duration t_{avg} is one hour, but can be lengthened up to two hours by ground command. The parameter T_{ex} is the proton temperature expected for quasi-stationary (CH and IS) wind with speed V_p. The ratio T_{ex}/T_p should average about 1 for CH and IS wind, but significantly exceed unity for CME wind. The calculation of T_{ex} is described in Sections 3 and 4. Running averages of V_p, N_p, and T_p are also calculated over the first and second halves of the interval t_{avg}. V_1 and V_2 are the first and second $t_{avg}/2$ values of the speed, and N_1, N_2, T_1, and T_2 are similarly defined averages of proton density and temperature.

In addition to addressing the persistence requirement, the averaging allows continued operation of the logic even when some parameters are temporarily missing. All ion data (V_p, T_p, N_p, and N_a) will be missing once every 20 data cycles when GIM performs its routine search mode, or when abrupt changes in speed trigger an additional search mode (Barraclough *et al.*, 2002). When T_p is unusually high, the alpha-particle peak in the spectrum cannot be discerned above the proton distribution, so N_a cannot be calculated. The GEM bidirectional streaming parameter B_e can be disabled when the angular distribution of electrons indicates that the spacecraft may be magnetically connected to the Earth's bow shock or when the GEM background becomes high during solar energetic particle events. The drawback of the averaging process is that whenever the regime changes, the wrong collector will be exposed for a time $t_{avg}/2$ prior to an array change. For 150 regime changes/year and t_{avg} = one hour, the wrong collector would be exposed an average of 0.9% of the time even if the algorithm otherwise worked perfectly.

The algorithm for determining the regime depends on whether or not a forward shock has recently passed the spacecraft. Shock passage

is deemed to have occurred when the following conditions are met:

$$V_2 - V_1 > V_{jump} \tag{1}$$

$$N_2/N_1 > R_N \tag{2}$$

$$T_2/T_1 > R_T \tag{3}$$

Nominal values of the constants are $V_{jump} = 40$ km/s, $R_N = 1.4$, and $R_T = 1.5$. These values were chosen to identify strong shocks with a very low rate of false alarms; weak shocks will not be detected. The time of the shock passage (t_{shock} = t_{now} - $t_{avg}/2$, where t_{now} is the current time) is saved.

The logical flow of the regime selection algorithm is diagrammed in Figure 1. At the start of the analysis, the current regime is denoted by a parameter LASTYPE = 0 (instrument startup), 1 (CME), 2 (CH), or 3 (IS). Suppose that LASTYPE $\neq$1; i.e., the regime is not CME. Whether or not the regime should be changed to CME depends on the parameter TOCME, whose derivation is shown in Figure 2. The CTn, CAn, and CBn are adjustable constants. Because, at a solar distance of 1 AU, almost all interplanetary shocks are driven by CMEs, we make it easier to enter the CME regime within a fixed time interval after t_{shock}. The boundaries of that time interval are determined by the uploadable parameters *ctime1* and *ctime2*, whose nominal values are 5 and 25 hours, respectively. Because alpha-particle and bidirectional electron streaming data will sometimes be missing, those parameters are assigned weights, W_a and W_b, respectively, which are 1 if there are data within the interval t_{avg}, and 0 if there are not. (No analysis is done if there are no values of either V_p or T_p within the time t_{avg}.) A simple fuzzy-logic scheme is used to combine the parameters T_{ex}/T_p, N_a/N_p, and B_e. As an example, Figure 3 shows how, for CA1 = 23, CA2 = 1.15, CA3 = 16.67, and CA4 = 1.0, the alpha-particle parameter Y_a depends on N_a/N_p for intervals that do and do not follow a shock. Similar diagrams could be drawn for Y_t and Y_b. TOCME is calculated from the weighted averages of Y_a, Y_t, and Y_b. If TOCME exceeds a threshold value (currently set at 0.4), the time of entering the CME is noted (as t_{cme}), LASTYPE is set to 1, and the collector arrays are changed to expose the CME array.

It is especially important not to allow the parameter Y_b alone to trigger a change into the CME regime. This is because true bidirectional electron streaming is sometimes found upstream of both forward and reverse shocks in corotating interaction regions (Gosling *et al.*, 1993) and because depletions in suprathermal electrons are sometimes observed at pitch angles of 90° (Gosling *et al.*, 2001) and these depletions

can be mistaken for CME-associated bidirectional streaming. We guard against false entry into the CME regime in two ways: (1) For the TOCME threshold greater than 1/3, more than one of the Y parameters must exceed 0 to trigger entry to the CME regime; e.g., if $Y_t = 1$ with Y_a and $Y_b = 0$, TOCME = 0.33 and the regime is not changed (2) Use of the sum $(2 + W_b)$ in the denominator of the expression for TOCME in Figure 2 (rather than $1 + W_a + W_b$) prevents bidirectional electron streaming alone from causing entry into CME mode even when the alpha-particle density could not be determined and W_a.

The trailing edges of CMEs are less well defined than are their leading edges (e.g., Neugebauer *et al.*, 1997). To protect the CH and IS collectors from CME wind, we make it harder to exit from the CME regime than it was to enter. The CME signatures often come and go within an event. The high helium abundance signature is notoriously patchy (Zwickl, 1983) and the bidirectional electron streaming feature can disappear as some of the solar field lines reconnect with the interplanetary magnetic field (Gosling *et al.*, 1995). For these reasons we require that a minimum time, t_{stay}, be spent in the CME regime. The current value of t_{stay} is 18 hours. After that time has elapsed, the CME regime is retained as long as any of the three signatures (N_a/N_p, T_{ex}/T_p or B_e) remains above their respective threshold values; currently, $A_{out} = 0.06$, $T_{out} = 1.5$, and $B_{out} = 0.4$. Persistence is provided by requiring the non-CME conditions to prevail for a time t_{lag} (currently 6 hours) before switching to either CH or IS.

Upon exiting the CME regime, the new regime is determined on the basis of the proton speed. If $V_p > V_c$, the new regime is CH; otherwise it is IS. Currently, V_c is set at 500 km/s.

Next, suppose Genesis is in the CH regime (LASTYPE = 2), TOCME is less than threshold, and the velocity starts decreasing. When V_p drops below V_{down} (currently 425 km/s), the regime changes to IS. It cannot return to the CH regime unless V_p subsequently increases above V_{up} (currently 525 km/s). This gap between V_{up} and V_{down} provides the required hysteresis. There is, however, a second requirement on changing from IS to CH to account for the fact that slow, IS wind that has been accelerated by an interplanetary shock has its source in the interstream wind, not in coronal holes. When an interplanetary shock is detected in an IS regime, the IS regime is held until either a CME is encountered or a time t_{sheath} (currently 12 hours) has elapsed.

3. Calculation of parameters used by the algorithm

As explained in the accompanying paper by Barraclough *et al.* (2002), GIM acquires a 3-dimensional array of counts at 40 energy channels (voltage levels) in 40 azimuth directions (angle φ) for each of 8 detectors (angle θ) every 2.5 minutes. These 12,800 count values are then checked for reasonableness and corrected for dead time and background level; the detailed logic of those operations is beyond the scope of this review. A three-dimensional phase space density $f_{3D}(v_p,\varphi,\theta)$ is then calculated in the usual way as $f_{3D}(v_p,\varphi,\theta) = 2\times\text{Counts}/(v_p^4 G\Delta\text{t})$, where $v_p = \sqrt{2(E/q)/m_p}$, m_p is the proton mass, E/q is the proton energy per unit charge, which is proportional to the voltage applied to the analyzer, G is a geometric factor, and Δt is the time over which counts are accumulated. At this stage of the calculation it is assumed that all counts are due to protons. Next, the matrix of 12,800 3-D values of phase space density are summed over all angles to yield a one-dimensional distribution function

$$f_{1D}(v_p) = \sum\sum v_p^2 f_{3D}(v_p,\varphi,\theta) sin(\theta)\Delta\varphi\Delta\theta. \tag{4}$$

This 1-D spectrum is then divided into a proton spectrum extending from $v_p = v_L$ to v_M and an alpha-particle spectrum extending from $v_p = v_M$ to v_H. Without going into the details, this process includes steps to ensure that the velocity bin with the highest value of $f_{1D}(v_p)$ is not an outlier, that a second (alpha-particle) peak exists at a reasonable number of velocity bins above the highest (proton) peak, and that the height of the alpha-particle peak is sufficiently above the minimum value between the two peaks. The limits v_L and v_H are the lowest and highest proton speeds in the 1-D spectrum and v_M is the proton speed at the minimum between the proton and alpha peaks. When it is not possible to find a reliable alpha-particle peak, v_M is set to a value of v_p 27% higher than the value of v_p for which $f_{1D}(v_p)$ reaches its peak, or that value for which $f_{1D}(v_p)$ is down to 2.5 % of its peak, whichever is smaller.

Moments are then calculated from the 1-D distribution function as follows:

$$N_p = \int_{v_L}^{v_M} f_{1D}(v_p) dv_p \tag{5}$$

$$N_a = \sqrt{2}\int_{v_M}^{v_H} f_{1D}(v_p) dv_p \tag{6}$$

$$V_p = [N_p]^{-1}\int_{v_L}^{v_M} v_p f_{1D}(v_p) dv_p \tag{7}$$

$$T_p = [m_p/kN_p] \int_{v_L}^{v_M} [v_p - V_p]^2 f_{1D}(v_p) dv_p \tag{8}$$

The resulting values of N_p, N_a, V_p, and T_p are then checked against uploadable sanity limits; for example, V_p must be between 200 and 1200 km/s for the data for that cycle to be included in the averages. As a final step in quality control, the moments' histories are despiked by the removal from the running averages of data from a single data cycle whose values are inconsistent with recent parameter trends.

In the quasi-stationary wind, the proton temperature increases with the proton speed. That unusually low temperatures are associated with transient solar wind events was recognized by Gosling *et al.* (1973). Richardson and Cane (1995) demonstrated that the decrease of the temperature well below a mean expected value (called T_{ex}) is a useful quantitative indicator of CMEs. A number of different fits have been made to different data sets to derive T_{ex} as a function of V_p. T_{ex} has variously been fit to a quadratic in V_p (Burlaga and Ogilvie, 1973), a linear function of V_p (Neugebauer *et al.*, 1997), or quadratic at low speed and linear at high speed ($>$ 500 km/s) (Lopez, 1987). To retain flexibility, we assume a relation of the form, for $V_p < V_{cut}$:

$$T_{ex} = C_1 + C_2 V_p + C_3 V_p^2 \tag{9}$$

and, for $V_p > V_{cut}$:

$$T_{ex} = C_4 + C_5 V_p + C_6 V_p^2 \tag{10}$$

At the start of the mission, we followed Richardson and Cane and used the constants derived from the relation developed from the NASA OMNI data set by Lopez (1987), for which V_{cut} = 500 km/s, C_1 = 26,000, C_2 = 316.2, C_3 = 0.961, C_4 = -142,000, C_5 = 510, and C_6 = 0 for V_p in km/s and T_{ex} in units of 10^3K. The form of this relationship is shown as the curve marked RC in Figure 4. As explained in Section 4, the constants were modified after analysis of the Genesis flight data.

The bidirectional electron streaming parameter B_e is calculated from the data acquired by GEM (Barraclough *et al.*, 2002). During a 2.5 minute data cycle, GEM obtains counts in each of 7 CEMs (polar angle) in 40 azimuth bins and 24 energy channels. The search for bidirectional streaming is limited to only an intermediate energy range for several reasons. The character of the core electron population at lower energies may be due to local effects rather than to the global field topology. At the highest energies the electrons provide too few counts per data cycle to yield statistically significant results. The energy range to be used can be changed by ground command, but a nominal range is the 12 energy channels between 160 and 984 eV. The counts are first

normalized by the geometric factor for each CEM and then summed over all CEMs to yield a 2-dimensional matrix in energy and azimuthal angle. Then, for each of the energy levels in the range of interest, the computer finds (1) the azimuth bin A_{peak} with the greatest number of counts C_{peak}, (2) C_{min}, which is the smaller of the number of counts averaged over bins near +90° and -90° from A_{peak}, and (3) C_{180}, which is the number of counts 180° from A_{peak}. Bidirectional streaming is deemed to be present at a given energy level if both C_{peak}/C_{min} and C_{180}/C_{min} exceed uploadable threshold values. A positive detection of bidirectional electron streaming (BDE) requires the presence of BDE behavior as outlined above in at least a minimum number of energy levels (nominally 3 or 4).

If the interplanetary magnetic field is approximately aligned with the spacecraft spin axis, bidirectional streaming would be evident in the polar, rather than in the azimuthal angular distribution. Therefore, if no BDE is found in the analysis of the azimuthal angles, a second search is done using the polar angles. The counts are again normalized according to geometric factor and then summed over azimuth for each relevant energy level. C_{min} is found by averaging over an uploadable list of CEMs (typically CEM#3 to CEM#5) and bidirectional streaming is deemed to be present for that energy level if both (Counts in CEM#1)/C_{min} and (Counts in CEM#7)/C_{min} exceed uploadable thresholds. As with the azimuthal search, BDEs must be detected in more than a minimum number of energy levels.

If bidirectional streaming is detected by analysis of either the azimuthal or the polar data, the parameter $B_e = 1$; otherwise, $B_e = 0$. When the interplanetary magnetic field connects the spacecraft to the region of the Earth's bow shock, bidirectional streaming may be caused by backstreaming of electrons accelerated at the shock, and thus give a false indication of CME conditions. For this reason, the BDE analysis can be disabled (the B_e weight W_b can be set to 0) if the polar direction of Earth is less than a threshold value (nominally 22°).

About twice a week during routine operations, the calculated moments and B_e together with compressed values of all the electron counts and a masked set of the ion counts for each data cycle are telemetered to the ground. Ground-based analyses determine the desirability of changing any of the parameters used in the on-board analyses. It is possible to adjust the computation of the moments and B_e to avoid using the counts acquired by any CEM that malfunctions.

4. In-Flight Performance

The regime-selection algorithm described in the previous sections was developed, and to the extent possible tested, using data from the ISEE-3 solar wind spectrometer measurements in 1978-1980. Additional, but necessarily limited testing was carried out before launch using dummy data. The first real test occurred during the first few months of the Genesis mission before the solar-wind collection began.

Following Genesis launch on August 8, 2001 and the spacecraft checkout period, GEM was turned on August 23 and GIM was turned on August 24. Since then, the operation of the monitors has met all expectations. During several large solar proton events, the background counts in GEM were too high (> 1000 counts per bin) to allow calculation of B_e, but the GIM background was much lower and the ion data were still usable.

The regime algorithm was activated on August 25. An error in the on-board geometric factors for GEM which prevented the proper operation of the search for bidirectional electron streaming was discovered and then corrected on September 19. On October 17, adjustments were made to the part of the algorithm that separates the alphas from the protons in the 1-D spectrum to improve the rejection of alpha-particle densities when the protons are too hot for a reliable identification of the alpha peak.

During the check-out period some excessive switching in and out of the CME regime was caused by the ephemeral nature of the CME signatures. This led to the addition of the parameter t_{lag} to the logical sequence as shown in Figure 1. This software change was implemented on December 13.

The values of the plasma moments calculated on-board from the 1-dimensional distribution functions have been compared to the moments calculated in the conventional manner from 3-dimensional data acquired by the SWEPAM instrument on the ACE spacecraft (McComas *et al.*, 1998). Figure 5 is a scatter plot of the proton speed calculated on Genesis versus the proton speed determined by ACE for the period August 24 to December 31, 2001. Only intervals with $V_p(\mathrm{ACE}) \geqslant 350$ km/s were included, thereby avoiding intervals for which ACE measurements have a somewhat larger uncertainty; intervals affected by solar energetic particles were also excluded. The time resolutions are 2.5 min for Genesis and 64 s for ACE. ACE measurements were interpolated to Genesis times, but no correction was made for the time shift (varying from 0 to 60 min) between features propagating past the two spacecraft. The correlation is excellent ($\mathrm{R} = 0.981$), and the on-board calculation of the

proton speed is deemed to be entirely adequate to meet the purposes of the regime algorithm.

Figure 6 shows a similar plot for the proton temperatures measured by Genesis and ACE. The Genesis temperatures are systematically higher than the ACE temperatures. The Genesis temperatures also appear to have a lower limit close to 10^4 K. The difference is caused by the different methods of calculation. On-board Genesis, the summations in Equation (4) extend over all angles, even those far from the part of the field of view that contains the peak of the distribution. Calculation of the ACE temperature, however, is limited to the part of phase space surrounding the peak of the distribution and is therefore less affected by the tail of the distribution and background counts. A result of the high temperatures calculated from Equations (4) and (8) is that T_{ex}/T_p was seldom greater than unity, even in some periods that were obviously CMEs. This situation was corrected by generating a new set of constants in Equations (9) and (10). First we fit 3 years of ACE speed and temperature data to find a T_{ex} relation for ACE; the results are given by the dashed curve in Figure 4. The data in Figure 6 were then fit to the relation $T_{Genesis} = 1.214 \times T_{ACE} + 6697$, and that relation was used to modify the T_{ex} calculated for ACE to yield a T_{ex}-V_p relation for Genesis. The resulting curve is shown as the heavy line in Figure 4. The new constants in Equation (9) and (10) are V_{cut} = 450 km/s, C_1 = -127800, C_2 = 595.2, C_3 = -0.1623, C_4 = -324400, C_5 = 1217, and C_6 = -0.5214 for V_p in km/s and T_{ex} in K.

The Sun was remarkably active in late 2001, resulting in many CMEs and interplanetary shocks. The Genesis shock-detection algorithm given in Equations (1) to (3) worked very well without any adjustments. Table 1 compares the shocks detected on-board Genesis with the shocks detected by the Proton Monitor of the Celias experiment on the SOHO spacecraft. (The SOHO shock list is available at the University of Maryland website at http://umtof.umd.edu/pm/). The Genesis shock passage times given in this table were obtained from the high-resolution (2.5-min) data obtained during the time t_{avg} preceding the on-board detection of the shock. Fourteen shocks were detected by both spacecraft. Genesis missed one weak shock that was observed by SOHO. No SOHO shocks corresponded to three of the Genesis shocks; at least two of those three were probably erroneous detections. Through November, the times of the Genesis shock passages followed the SOHO passages by 5 to 32 minutes because Genesis was still moving out to the L1 point and was downstream of SOHO. For the December shocks, both spacecraft were in halo orbits around L1 and the times agreed within the 0.5-min resolution of SOHO and the 2.5-min resolution of

Genesis. Further studies of shocks and other structures in the solar wind will be carried out through more detailed comparisons of data from Genesis, SOHO, and ACE.

Figures 7 and 8 provide examples of the operation of the regime algorithm during two different intervals. From top to bottom, the panels show (a) V_p, (b) T_p, (c) T_{ex}/T_p, (d) N_a/N_p, (e) the azimuthal distribution of suprathermal electrons over the energy range 243 to 298 eV, (f) B_e, (g) the parameter TOCME, and (h) the regime deduced from the data. Individual 2.5-min values are plotted in black and the running hourly averages are plotted in red. The data shown in panel (c) are the values of T_{ex}/T_p based on the Richardson-Cane equation for T_{ex} in use at the time the data were acquired; the revised equation for T_{ex}, which was not yet in use, would be higher.

Figure 7 shows the entry into and exit from a rather small CH stream. No shock was detected during that interval. For most of the CH interval, the helium abundance ratio N_a/N_p agreed with expectations for coronal hole flow, thereby corroborating our choice of a value for V_{up}. During the early Genesis period, there were no CH streams with the long durations and very high speeds typical of periods of declining solar activity.

A period that includes a CME is shown in Figure 8. Detection of a forward shock on day 294 is indicated by a vertical line. The regime before the shock was IS and it remained IS despite the high speed because of the $t_{sheath} = 12$ hr requirement. The regime changed to CME near day 294.8 on the basis of a strong onset of bidirectional electron streaming together with a small rise in T_{ex}/T_p. A helium enhancement and a much stronger temperature depression (high T_{ex}/T_p) soon followed. At day 295.93, the regime changed from CME to CH on the basis of the running averages of $T_{ex}/T_p = 1.42$, $N_a/N_p = 0.069$, $B_e = 0.17$, and $V_p = 516$ km/s; the values of T_{out}, A_{out}, and B_{out} in use at the time were 1.5, 0.07, and 0.4, respectively. T_{ex}/T_p started to rise almost immediately thereafter, but TOCME did not reach the threshold value of 0.4 required to reenter the CME regime until day 296.06. In retrospect, we think that CME conditions may have prevailed essentially continuously from day ∼294.8 until day ∼297.8. The algorithm would have held the CME regime without the short excursion into CH if the t_{lag} part of the logic had been in place at the time.

5. Conclusions

We have developed and flight-tested an algorithm for determining the flow regime (coronal hole, interstream, or coronal mass ejection) of the

solar wind on the basis of running hourly averages of solar wind ion and electron parameters. After a few adjustments, the performance of the algorithm has turned out to be generally satisfactory While the algorithm now makes few blatant errors, its success rate is difficult to quantify at this point.

To protect the cleanliness of the CH bin we have modified some parts of the software and some parameters to tighten up the exclusion of CME wind from the CH regime. We will continue to monitor the regime idenfications throughout the mission, not only by examining the Genesis GIM and GEM data alone, but by comparing it to nearly simultaneous data acquired by ACE. The ACE composition data are expected to be particularly useful in identifying stream interfaces between IS and CH flows. As a result of further analyses, we may adjust the parameters V_{up} or V_{down} to minimize mixing of the CH and IS regimes. At the end of the mission we will estimate the cross-contamination of each of the regimes by the other two. Because CMEs are often difficult to identify even under the best of circumstances with many more data types than are available on Genesis, perfection should not be expected.

We note in closing that similar algorithms might be useful in several other contexts.

Acknowledgements

Part of this work was performed at the Jet Propulsion Laboratory (JPL) of the California Institute of Technology under a contract with the National Aeronautics and Space Administration (NASA). The work at Los Alamos was performed under the auspices of the U. S. Department of Energy under NASA contract W-19,272. The work at Lockheed Martin was performed under a contract from JPL. We thank F. Ipavich for providing the Celias proton monitor data from the Solar Heliospheric Observatory (SOHO); SOHO is a joint European Space Agency and NASA mission.

References

Barraclough, B. L., *et al.: 2002, 'The plasma ion and electron instruments for the Genesis mission', Space Sci. Rev., this volume.*

Burlaga, L. F., and Ogilvie, K.W.: 1973, 'Solar wind temperature and speed', J.Geophys.Res., **78**, *2028.*

Burnett, D. S., et al.: 2002, 'The Genesis Discovery mission: Return of solar matter to Earth', Space Sci. Rev., this volume.

Galvin, A. B.: 1997, 'Minor ion composition in CME-related solar wind', in Coronal Mass Ejections, Geophysical Monograph 99, edited by N. Crooker, J. A. Joselyn and J. Feynman, pp. 253, Amer. Geophys. Un., Washington, DC.

Gloeckler, G., Fisk, L.A., Hefti, S., Schwadron, N. A., Zurbuchen. T.H., Ipavich, F.M., Geiss, J., Bochsler, P., and Wimmer-Schweingruber, R.F.: 1999, 'Unusual composition of the solar wind in the 2-3 May 1998 CME observed with SWICS on ACE', Geophys.Res.Lett., **26**, *157.*

Gosling, J.T., Pizzo, V., and Bame, S.J.: 1973, 'Anomalously low proton temperatures in the solar wind following interplanetary shock waves: Evidence for magnetic bottles?', J.Geophys.Res., **78**, *2001.*

Gosling, J. T., Bame, S. J., Feldman, W.C., McComas, D. J., Phillips, J. L., and Goldstein, B. E.: 1993, 'Counterstreaming suprathermal electron events upstream of corotating shocks in the solar wind beyond 2 AU: Ulysses', Geophys.Res.Lett., **20**, *2335.*

Gosling, J. T., Birn, J., and Hesse, M.: 1995, 'Three-dimensional magnetic reconnection and the magnetic topology of coronal mass ejection events', Geophys.Res.Lett., **22**, *869.*

Gosling, J. T., Skoug, R. M., and Feldman, W. C.: 2001, 'Solar wind electron halo depletions at 90 deg pitch angles', Geophys.Res.Lett., **28**, *4155.*

Ho, G. C., Hamilton, D. C., Gloeckler, G., and Bochsler, P., 2000, 'Enhanced solar wind $^3He^{2+}$ *associated with coronal mass ejections', Geophys.Res.Lett.*, **27**, *309.*

Lopez, R.E.: 1987, 'Solar cycle invariance in the solar wind proton temperature relationships', J.Geophys.Res., **92**, *11189.*

McComas, D. J., et al.: 1998, 'Solar wind electron proton alpha monitor (SWEPAM) for the Advanced Composition Explorer', SpaceSci.Rev., **86**, *563.*

Neugebauer, M., Goldstein, R., and Goldstein, B.E.: 1997, 'Features observed in the trailing regions of interplanetary clouds from coronal mass ejections', J.Geophys.Res., **102**, *19.*

Richardson, I. G., and Cane, H.V.: 1995, 'Regions of abnormally low proton temperature in the solar wind (1965-1991) and their association with ejecta', J.Geophys.Res., **100**, *23,397.*

von Steiger, R., Schwadron, N.A., Fisk, L.A., Geiss, J., Gloeckler, G., Hefti, S., Wilken, B., Wimmer-Schweingruber, R.F., and Zurbuchen, T.H.: 2000, 'Composition of quasi-stationary solar wind flows from Ulysses/Solar Wind Ion Composition Spectrometer', J.Geophys.Res., **105**, *27217.*

Zwickl, R. D., Asbridge, J.R., Bame, S.J., Feldman, W.C., Gosling, J.T., and Smith, E.J.: 1983, 'Plasma properties of driver gas following interplanetary shocks observed by ISEE-3', in Solar Wind Five; NASA Conference Proceedings 2280, edited by M. Neugebauer, pp. 711, NASA, Washington, DC.

Figure Captions

Figure 1. Logical flow of the regime-selection algorithm

Figure 2. Expanded view of the logic that combines the proton temperature, helium abundance, and bidirectional streaming parameters to determine the likelihood of wind from a coronal mass ejection. The W_a and W_b are relative weights of the helium abundance and bidirectional streaming parameters based on the number of valid determinations over the averaging interval.

Figure 3. Illustration of the calculation of the parameter Y_a (used in Figure 2) from the helium abundance ratio N_a/N_p.

Figure 4. Comparison of three expressions for the dependence of expected proton temperature T_{ex} on solar wind speed. RC is the expression used by Richardson and Cane for identification of CMEs. ACE is the expression derived from three-years of ACE data. The heavy curve is the value used for Genesis based on the ACE T_{ex}-V curve adjusted for the fact that Genesis measures higher proton temperatures than does ACE.

Figure 5. Scatter plot of the nearly simultaneous proton speeds observed by Genesis and ACE.

Figure 6. Scatter plot of the nearly simultaneous proton temperatures observed by Genesis and ACE.

Figure 7. Example of Genesis identification of a solar wind stream from a coronal hole. From top to bottom are plotted (a) proton speed V_p, (b) proton temperature T_p, (c) the ratio of the expected temperature to the observed temperature, (d) the helium abundance ratio N_a/N_p, (e) the azimuthal angular distribution of electrons in the energy range 243 to 298 eV, (f) the bidirectional streaming parameter B_e, (g) the TOCME parameter , and (h) the regime selected. In each panel except (e), the black points are the instantaneous 2.5-minute values and the red points are the hourly running averages.

Figure 8. Example of Genesis identification of a solar wind stream associated with a coronal mass ejection. The panels are the same as those in Figure 7.

Table I. Times of interplanetary shocks

	UT Time	
Date	SOHO	Genesis
08/27/01	19:14	19:30
08/30/01	13:26	13:38
09/01/01	Not listed	02:33[1]
09/14/01	01:08	01:22
09/25/01	19:51	20:09
09/29/01	09:03	09:10
09/30/01	18:41	18:48
10/11/01	16:13	16:25
10/21/01	16:05	16:13
10/25/01	07:57	08:29
10/28/01	02:33	02:38
10/31/01	12:49	13:14
11/06/01	01:20	Monitors Off
11/06/01	Not Listed	16:30[2]
11/15/01	13:45	Not Detected[3]
11/19/01	17:34	17:46
11/24/01	05:33	Monitors Off
12/17/01	Not Listed	03:07[4]
12/29/01	04:56	04:58
12/30/01	19:38	19:39

[1] Looks like a weak shock in the plasma parameters, but the ACE magnetometer shows the field strength decreasing rather than increasing. Probably a bad detection.
[2] Not a clean shock signature; embedded within a fast CME.
[3] Weak shock not found by shock-detection algorithm but visible in data.
[4] Appears to be a forward wave which has not steepened into a shock.

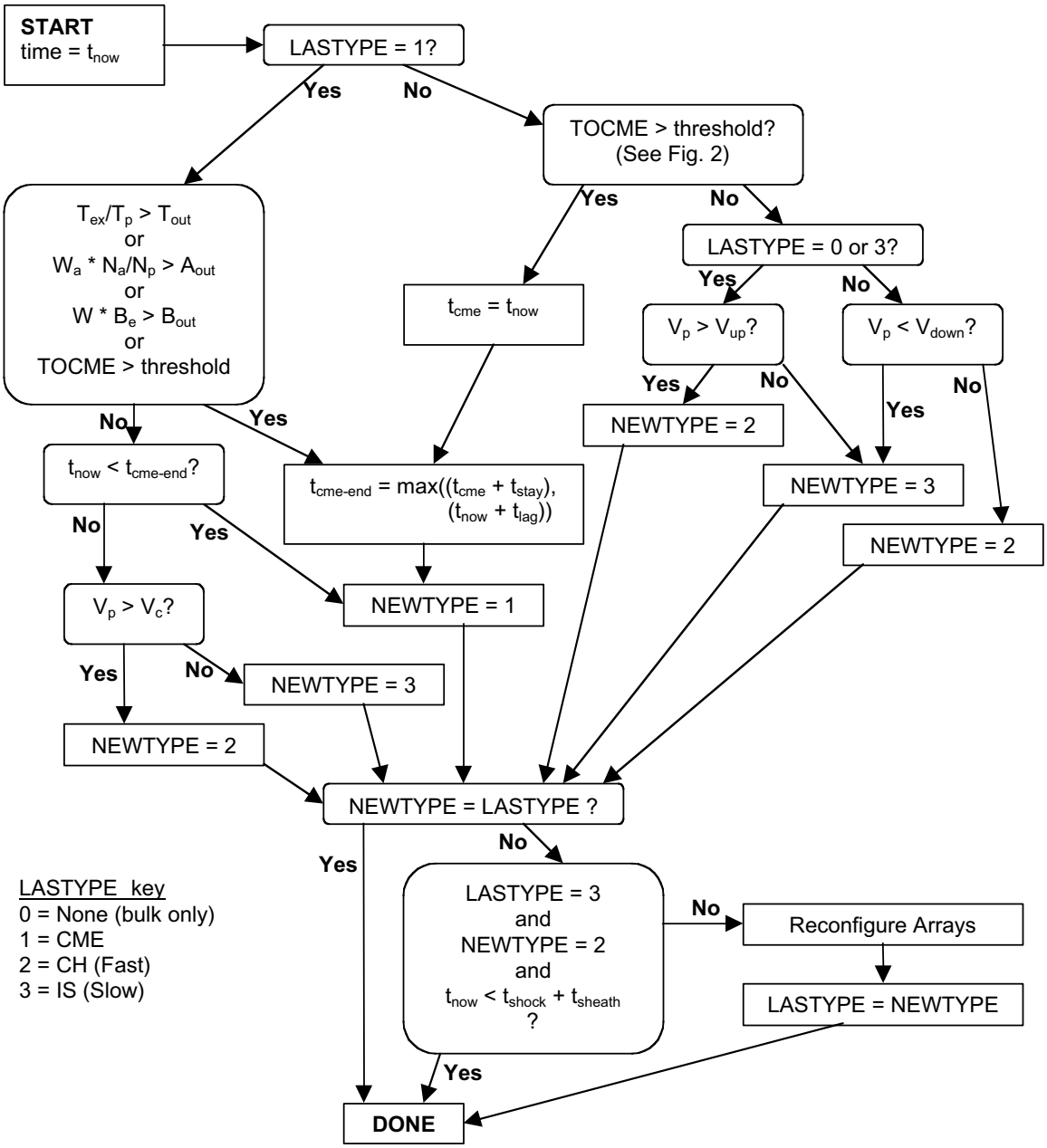
START
time = t_{now}
LASTYPE = 1?
Yes
No
TOCME > threshold?
(See Fig. 2)
$T_{ex}/T_p > T_{out}$
or
$W_a * N_a/N_p > A_{out}$
or
$W * B_e > B_{out}$
or
TOCME > threshold
$t_{cme} = t_{now}$
LASTYPE = 0 or 3?
$V_p > V_{up}$?
$V_p < V_{down}$?
NEWTYPE = 2
NEWTYPE = 3
NEWTYPE = 2
$t_{now} < t_{cme-end}$?
$t_{cme-end} = max((t_{cme} + t_{stay}), (t_{now} + t_{lag}))$
$V_p > V_c$?
NEWTYPE = 1
NEWTYPE = 3
NEWTYPE = 2
NEWTYPE = LASTYPE ?
LASTYPE = 3
and
NEWTYPE = 2
and
$t_{now} < t_{shock} + t_{sheath}$
?
Reconfigure Arrays
LASTYPE = NEWTYPE
DONE
LASTYPE key
0 = None (bulk only)
1 = CME
2 = CH (Fast)
3 = IS (Slow)

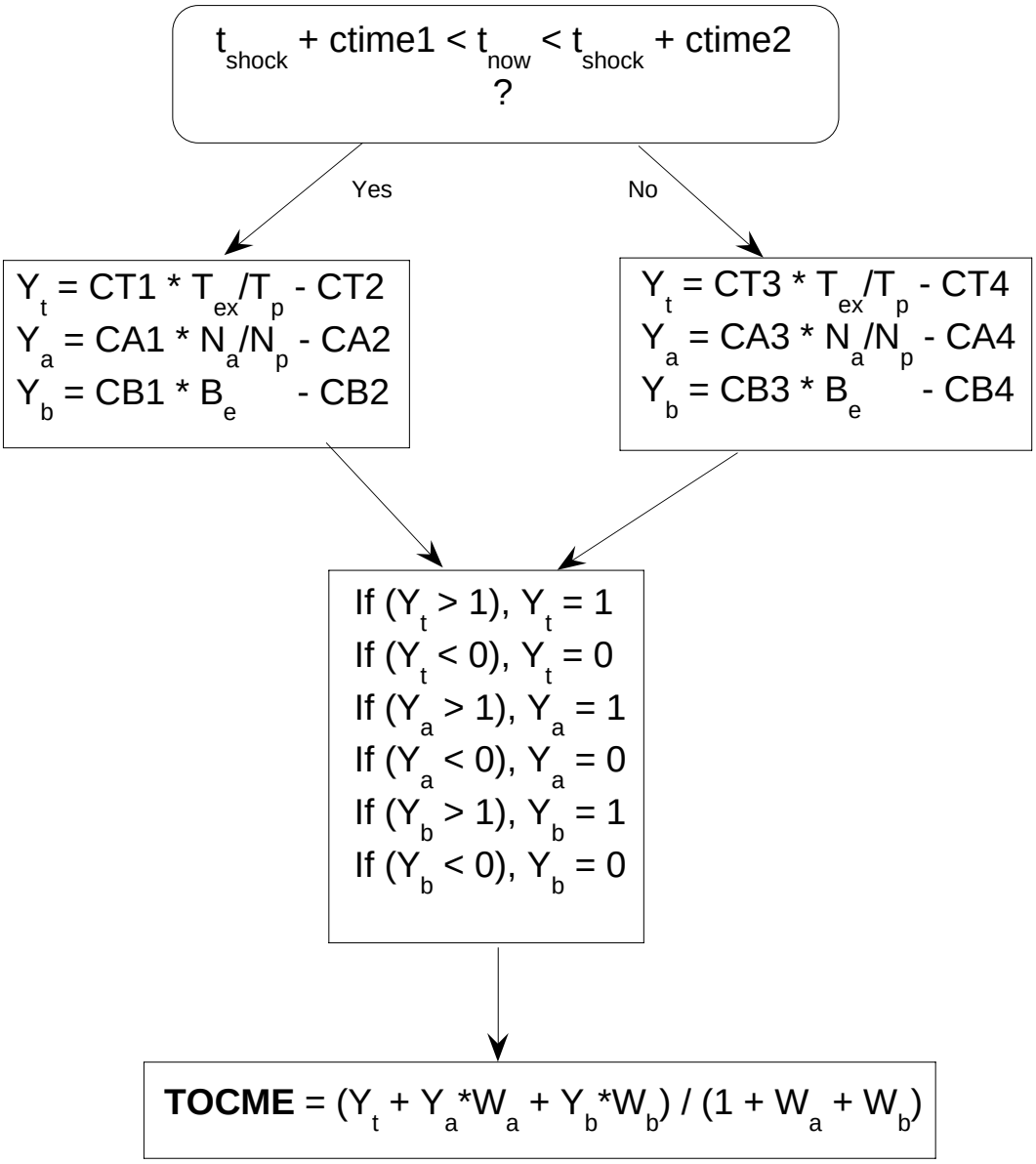
$t_{shock} + ctime1 < t_{now} < t_{shock} + ctime2$?
Yes
No
$Y_t = CT1 * T_{ex}/T_p - CT2$
$Y_a = CA1 * N_a/N_p - CA2$
$Y_b = CB1 * B_e - CB2$
$Y_t = CT3 * T_{ex}/T_p - CT4$
$Y_a = CA3 * N_a/N_p - CA4$
$Y_b = CB3 * B_e - CB4$
If ($Y_t > 1$), $Y_t = 1$
If ($Y_t < 0$), $Y_t = 0$
If ($Y_a > 1$), $Y_a = 1$
If ($Y_a < 0$), $Y_a = 0$
If ($Y_b > 1$), $Y_b = 1$
If ($Y_b < 0$), $Y_b = 0$
TOCME = $(Y_t + Y_a*W_a + Y_b*W_b) / (1 + W_a + W_b)$

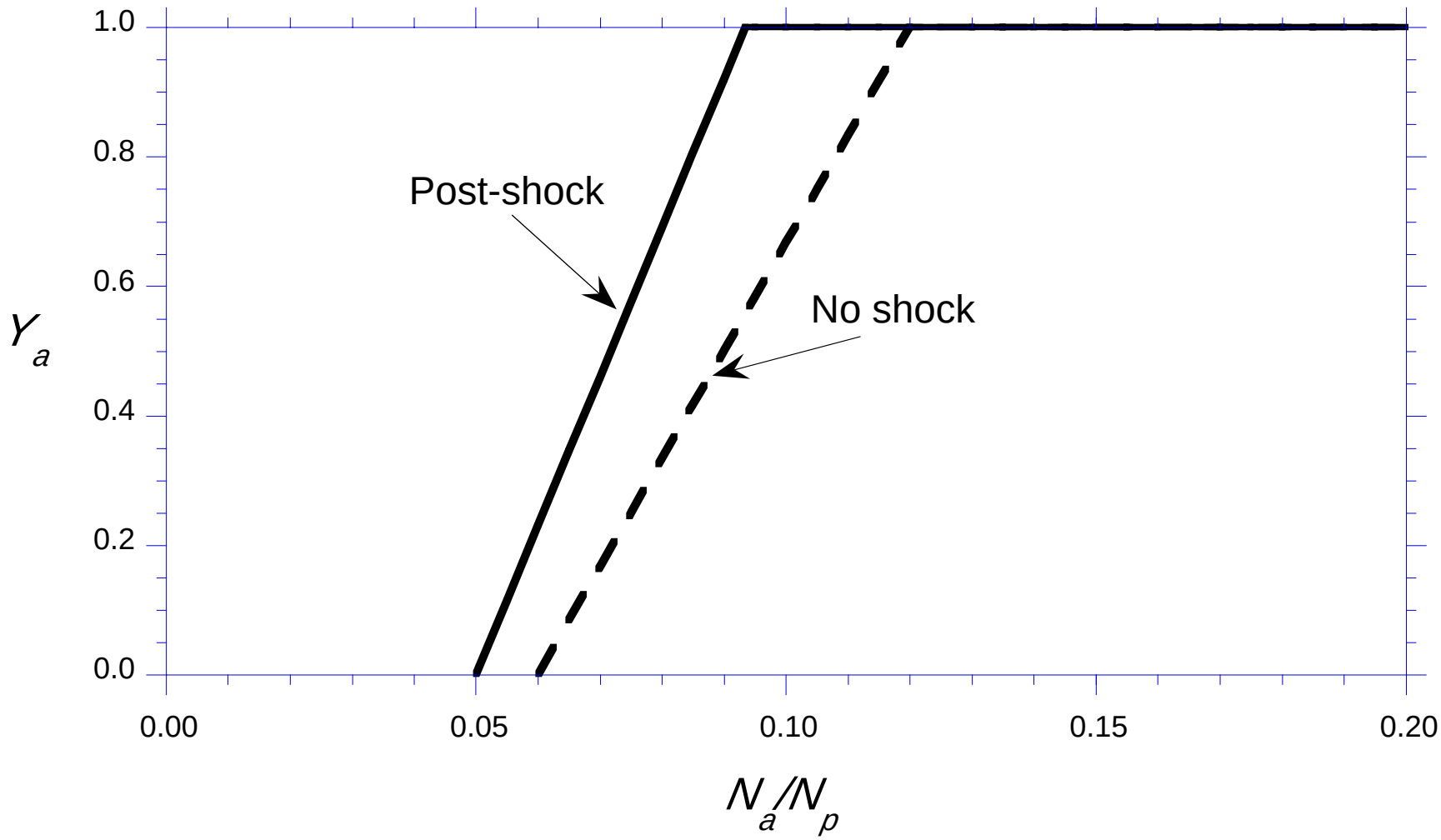
1.0
0.8
0.6
0.4
0.2
0.0
Y_a
Post-shock
No shock
0.00
0.05
0.10
0.15
0.20
N_a/N_p

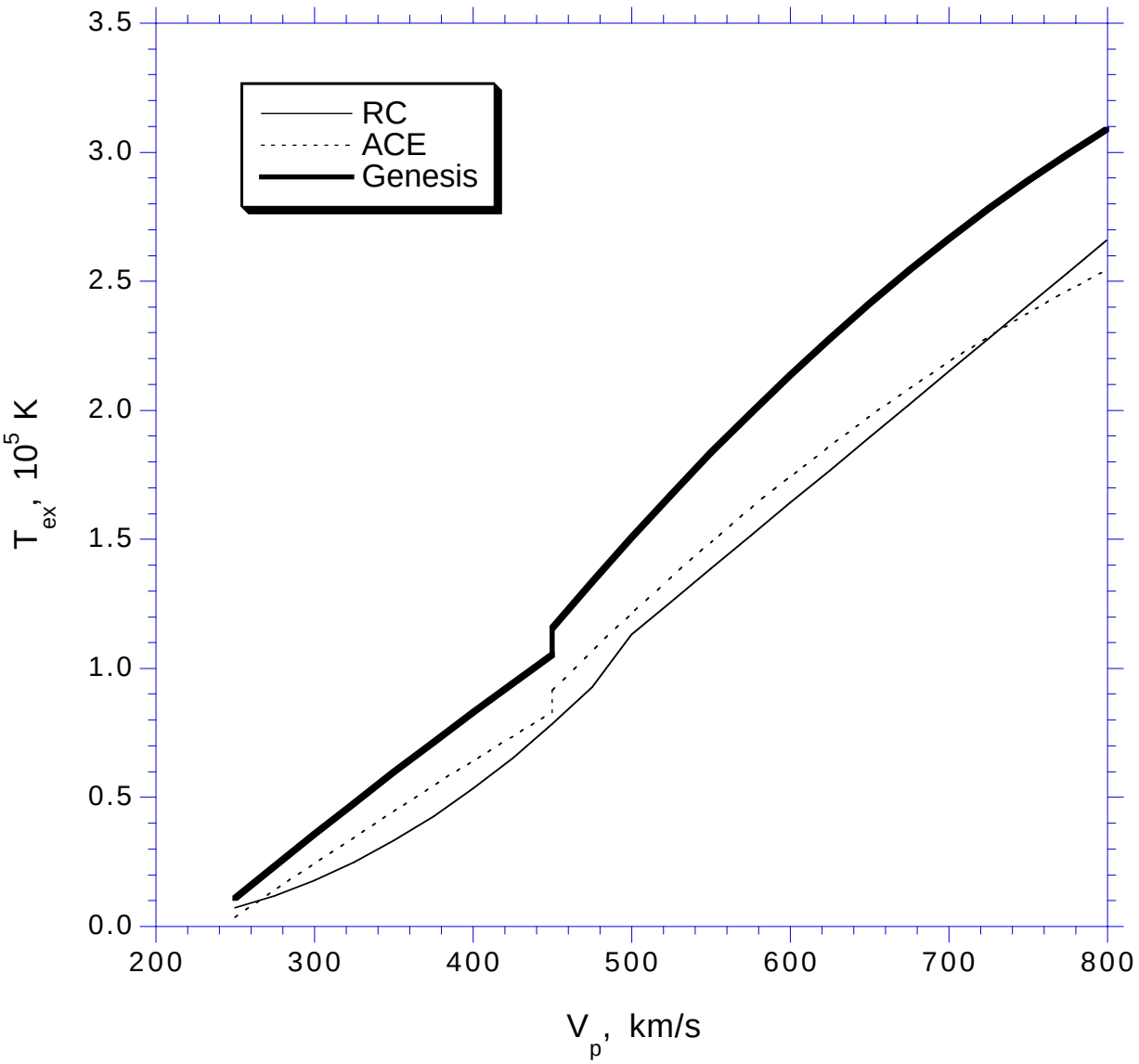
RC
ACE
Genesis
3.5
3.0
2.5
2.0
1.5
1.0
0.5
0.0
200
300
400
500
600
700
800
T_ex, 10^5 K
V_p, km/s

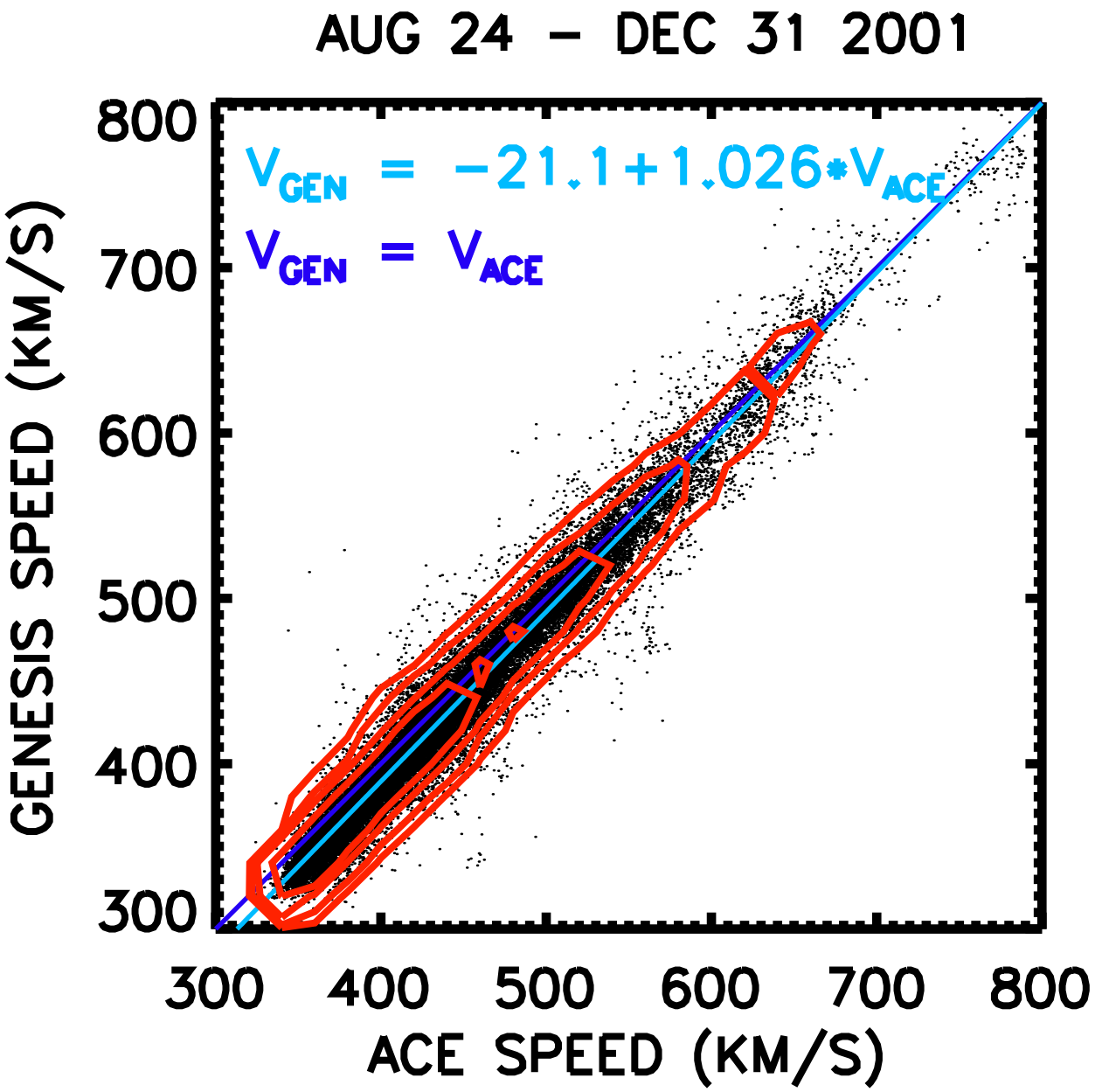
AUG 24 – DEC 31 2001
$V_{GEN} = -21.1 + 1.026 * V_{ACE}$
$V_{GEN} = V_{ACE}$
GENESIS SPEED (KM/S)
ACE SPEED (KM/S)
300
400
500
600
700
800

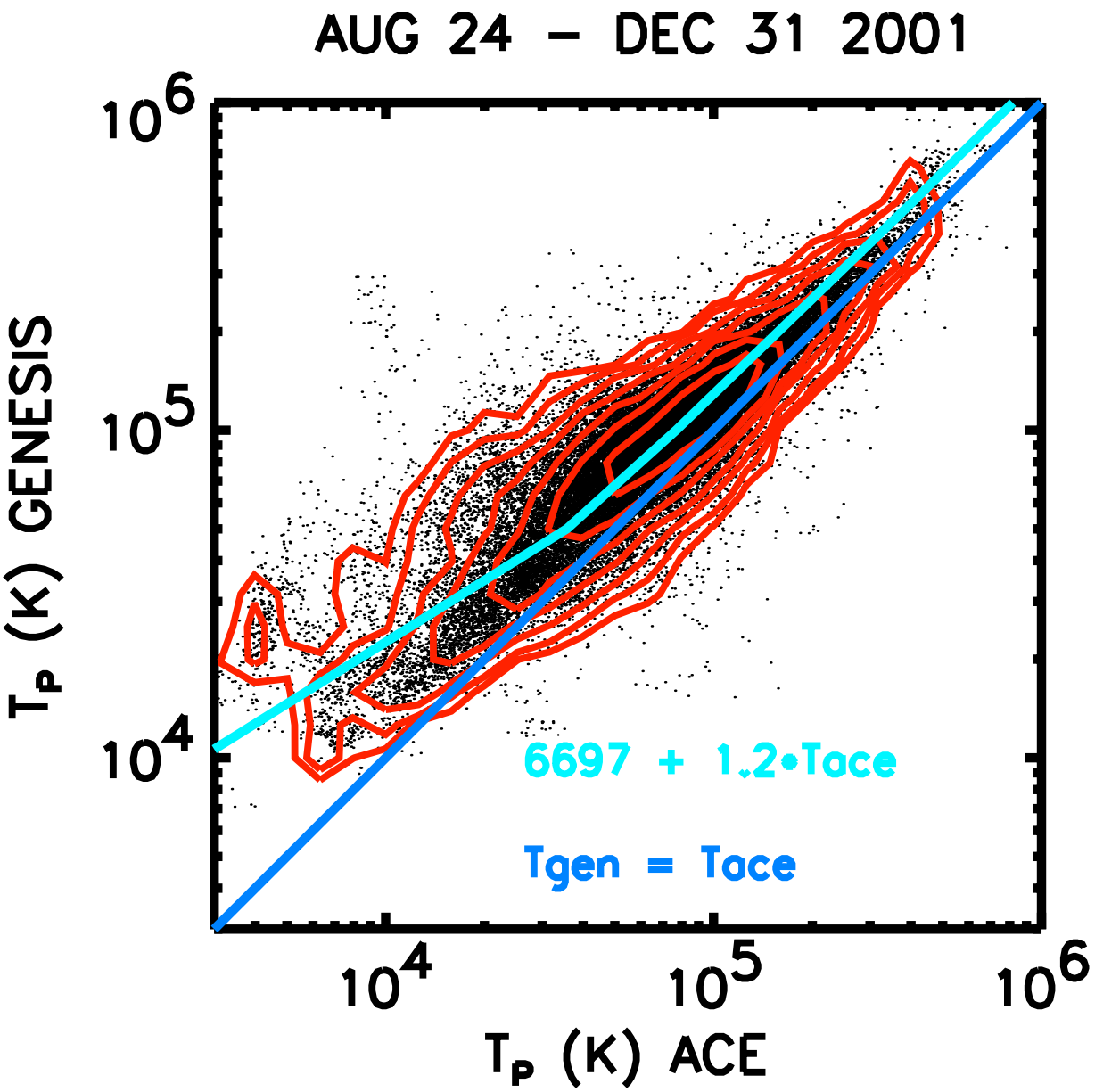
AUG 24 – DEC 31 2001
10^6
10^5
10^4
T_P (K) GENESIS
6697 + 1.2•Tace
Tgen = Tace
10^4
10^5
10^6
T_P (K) ACE

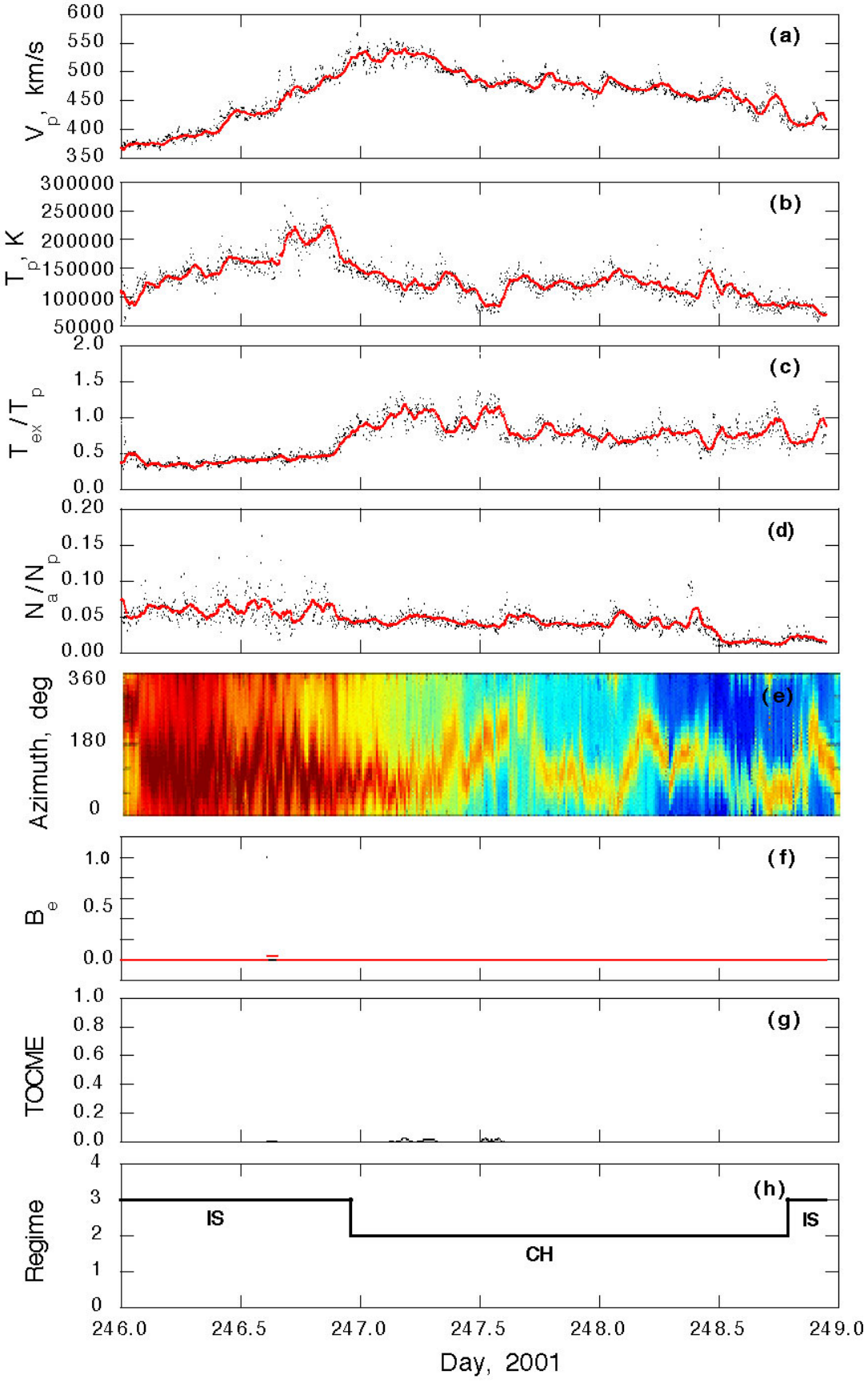
(a)
V_p, km/s
600
550
500
450
400
350
(b)
T_p, K
300000
250000
200000
150000
100000
50000
(c)
T_{ex}/T_p
2.0
1.5
1.0
0.5
0.0
(d)
N_a/N_p
0.20
0.15
0.10
0.05
0.00
(e)
Azimuth, deg
360
180
0
(f)
B_e
1.0
0.5
0.0
(g)
TOCME
1.0
0.8
0.6
0.4
0.2
0.0
(h)
Regime
4
3
2
1
0
IS
CH
IS
246.0
246.5
247.0
247.5
248.0
248.5
249.0
Day, 2001

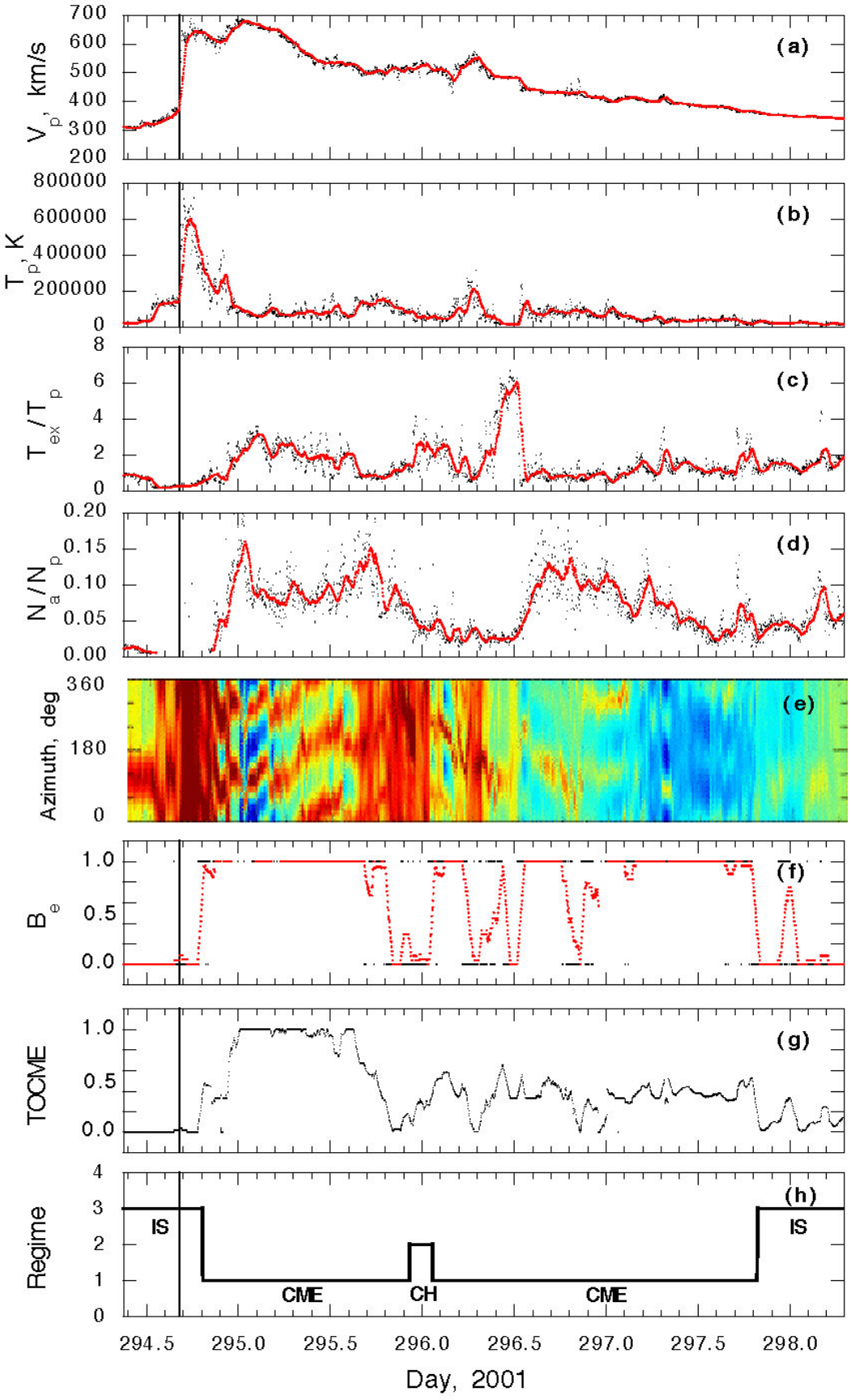
(a)
V_p, km/s
700
600
500
400
300
200
(b)
T_p, K
800000
600000
400000
200000
0
(c)
T_{ex}/T_p
8
6
4
2
0
(d)
N_a/N_p
0.20
0.15
0.10
0.05
0.00
(e)
Azimuth, deg
360
180
0
(f)
B_e
1.0
0.5
0.0
(g)
TOCME
1.0
0.5
0.0
(h)
Regime
4
3
2
1
0
IS
CME
CH
CME
IS
294.5
295.0
295.5
296.0
296.5
297.0
297.5
298.0
Day, 2001